JCTC Journal of Chemical Theory and Computation

Article

pubs.acs.org/JCTC

First-Principles Investigation of Strong Excitonic Effects in Oxygen 1s X-ray Absorption Spectra

Yoshifumi Noguchi,*[,†] Miyabi Hiyama,[†] Hidefumi Akiyama,[†] Yoshihisa Harada,[†] and Nobuaki Koga[‡]

[†]Institute for Solid State Physics, The University of Tokyo, 5-1-5 Kashiwanoha, Kashiwa, Chiba 277-8581, Japan

[‡]Graduate School of Information Science, Nagoya University, Furo-cho, Chikusa-ku, Nagoya 464-8601, Japan

Supporting Information

ABSTRACT: We calculated the oxygen 1s X-ray absorption spectra (XAS) of acetone and acetic acid molecules in vacuum by utilizing the first-principles *GW* +Bethe−Salpeter method with an all-electron mixed basis. The calculated excitation energies show good agreement with the available experimental data without an artificial shift. The remaining error, which is less than 1% or 2−5 eV, is a significant improvement from those of time-dependent (TD) density functional methods (5% error or 27−29 eV for TD-LDA and 2.4−2.8% error or 13−15 eV for TD-B3LYP). Our method reproduces the first and second isolated peaks and broad peaks at higher photon energies, corresponding to Rydberg excitations. We observed a failure of the one-particle picture (or independent particle approximation) from our assignment of the five lowest exciton peaks and significant excitonic or state-hybridization effects inherent in the core electron excitations.

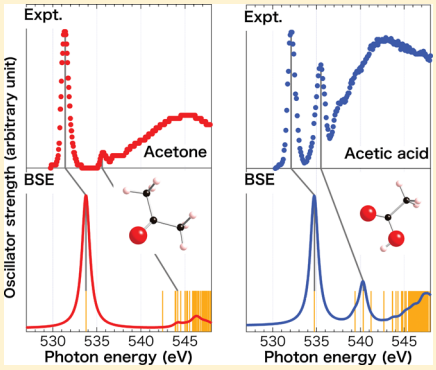

INTRODUCTION

X-ray absorption spectra (XAS), in which the targeting photon energy reaches more than a few hundred electron volts, include a great deal of helpful information on the electronic structures and local atomic geometries of the material.[1] Recent developments in experimental techniques enable us to obtain sufficiently accurate XAS and discuss the electronic and atomic properties of a wide range of materials under various experimental conditions.[2] Detailed analysis of the obtained XAS requires theoretical background to acquire the most useful insights. Consequently, collaboration between experiment and theory is becoming more important. A *fully* first-principles method that is capable of not only simulating promising XAS but also providing reliable interpretation for experimental XAS without requiring artificial factors is strongly desired. Nevertheless, first-principles development other than the total-energy-difference method, which is based on an assumption that the one-particle picture (or independent particle approximation) works well, seems to have stagnated over the last few decades.[3−8]

We first review previous XAS efforts to illustrate the current capabilities of theoretical studies. Modern theoretical tools for simulating photoabsorption spectra explicitly deal with the excitonic effect and are based on the two-particle picture because, at least for valence electron excitations in the low photon energy range corresponding to UV−vis spectra, a failure of the one-particle picture is commonly recognized. Time-dependent density functional theory (TDDFT) is a well-established method for simulating valence electron excitations. Furthermore, TDDFT with a semiempirical hybrid exchange−correlation potential enables us to consider deep-core electron excitation as well.[9−11]

Similar to TDDFT, a more advanced method that will enable us to simulate promising excited-state properties is the *GW* +Bethe−Salpeter method based on many-body perturbation theory.[12−15] The *GW*+Bethe−Salpeter method solves the Bethe−Salpeter equation (BSE)[16,17] within the *GW* approximation (GWA).[18] Shirley first succeeded in explaining core−hole multieffects using the Anderson impurity model within BSE.[19,20] Later, Shirley, Rehr, and co-workers applied the *GW* +Bethe−Salpeter method combined with the pseudopotential method to some extended materials. They successfully replicated relative peak positions and peak shapes that are comparable with experimental XAS results.[21−26]

The successful studies by Shirley, Rehr, and co-workers encouraged us to develop a *fully* first-principles *GW*+Bethe−Salpeter method combined with an all-electron method that is capable of simulating the main features of deep-core excitations and analyzing the details of experimental XAS. The all-electron mixed-basis approach[27] using both plane waves (PWs) and numerical atomic orbitals (AOs)[28] could be a predominant candidate capable of accurately describing the complete electronic structure from the core- to free-electron states within realistic computational costs.[29−33] Moreover, combining the all-electron mixed-basis approach with the *GW*+Bethe−Salpeter method provides a proficient method not only for simulating XAS but also for assigning each exciton composing the spectra without requiring any adjustable parameters.

In this paper, we demonstrate a first-principles oxygen 1s XAS simulation for acetone and acetic acid by employing the *GW*+Bethe−Salpeter method and the all-electron mixed-basis

Received: November 20, 2014
Published: March 17, 2015

DOI: 10.1021/acs.jctc.5b00082
J. Chem. Theory Comput. 2015, 11, 1668−1673

approach for the first time. We determine the peak positions and the peak heights from first principles and directly compare the results to experimental spectra without any adjustment shifts. We analyze the experimental first and second isolated peaks involving a few individual excitons in detail and discuss the differences with conventional assignments based on the one-particle picture. In particular, the strong excitonic effect involving the oxygen 1s level is discussed in this study. The same type of discussion might be possible in high-level quantum chemistry calculations, such as configuration interaction and the equation-of-motion coupled-cluster method[34] employing an AO-only basis set if the basis set problem is negligibly small.[35] However, the present method has advantages in regard to computational cost and applicability because a wide range of materials, including both isolated and periodic systems, can be treated using the present method. As already recognized in the case of valence electron excitation, the two-particle-picture-based method explicitly dealing with the excitonic effect is crucial for simulating core electron excitations as well.

COMPUTATIONAL DETAILS

Because the details of our *GW*+Bethe−Salpeter method are given in refs 12−14, we only briefly explain our method here. Our method is primarily composed of three parts: First, a conventional DFT−local density approximation (LDA) calculation is performed, in which the DFT Hamiltonian can be regarded as the unperturbed term in the present method. Second, a *GW* calculation is performed to obtain the single-excitation (or *GW* quasiparticle) energies:

$$E_\nu^{GW} = E_\nu^{\mathrm{LDA}} + Z_\nu \langle \nu | \Sigma^{GW} - \mu_{\mathrm{xc}}^{\mathrm{LDA}} | \nu \rangle \tag{1}$$

in which

$$\Sigma^{GW} = \mathrm{i}GW \tag{2}$$

and

$$Z_\nu = \frac{1}{1 - \langle \nu | \partial \Sigma^{GW} / \partial E_\nu^{\mathrm{LDA}} | \nu \rangle} \tag{3}$$

where E_ν^{LDA} is the LDA Kohn−Sham orbital energy of the νth level, $\mu_{\mathrm{xc}}^{\mathrm{LDA}}$ is the LDA exchange−correlation potential, G is the one-particle Green's function, W is the dynamically screened Coulomb interaction within a random phase approximation (RPA), and Z is a renormalized factor. Finally, to consider the excitonic effect, we construct the BSE using the *GW* quasiparticle energies and solve the BSE within the GWA via the following eigenvalue problem:

$$(E_e^{GW} - E_o^{GW})\delta_{o,o'}\delta_{e,e'}A_{e,o}^S + \sum_{e',o'} \Xi_{e,o;e',o'}^{GW}(\Omega_S) A_{e',o'}^S = \Omega_S A_{e,o}^S \tag{4}$$

in which

$$\Xi^{GW} = \frac{\partial}{\partial G}(\Sigma^H + \Sigma^{GW}) \tag{5}$$

where the indices e and o refer to the empty and occupied levels, respectively, Ξ^{GW} is an electron−hole interaction kernel within GWA, and Σ^H and Σ^{GW} are the Hartree and *GW* self-energy operators, respectively. (It should be noted that the Ω dependence in eq 4 is a result of an analytically performed ω integral to consider the dynamical effect and that the higher-order term of Ξ^{GW}, $\mathrm{i}G(\partial W/\partial G)$, is omitted in this study as well as in the usual procedure of the *GW*+Bethe−Salpeter method. The details are given in ref 14.) Because the excitonic effect is explicitly treated through Ξ^{GW} in eq 5 and eq 4 is diagonalized, the resulting eigenvalues Ω_S and eigenvectors A^S in eq 4 give us the excitonic properties based on the two-particle picture. By applying the all-electron mixed basis in eqs 1−5, we can simulate XAS as well as the UV−vis absorption spectra from first principles within the same framework using the same program code. In addition, in principle our method can also simulate the XAS of extended systems if we implement multiple k points in the program code.

We use a sufficiently large face-centered-cubic supercell, of which the length of the cubic edge is about 28.3 Å. We also use the Coulomb cutoff technique[36,37] to completely eliminate Coulomb interactions between molecules located in different supercells. To date our program code is unable to consider the effect of spin−orbit coupling; however, we consider the effect up to scalar relativistic levels by including the mass velocity and the Darwin terms. We describe the electronic states with a PW cutoff energy of 487 eV for both molecules. In the *GW* and Bethe−Salpeter calculations, we estimate the Fock exchange term and the bare Coulomb interaction with **G** vector cutoff energies of 940 eV for acetone and 2114 eV for acetic acid. We also estimate the *GW* correlation term and dynamic Coulomb interaction with **G** (**G**′) vector cutoff energies of 217 eV for acetone and 295 eV for acetic acid. Finally, 14400 empty levels for acetone and 12000 empty levels for acetic acid are summed in the calculation of the *GW* correlation term. In this study, we demonstrate that the *GW*+Bethe−Salpeter calculation combined with the all-electron mixed-basis approach using both PWs and AOs can successfully achieve *fully* first-principles calculations of XAS. The present *GW*+Bethe−Salpeter calculation required about 44 h for acetone and 64 h for acetic acid using 16 Intel Xeon E5-2697 v2 CPUs. This computational cost is much higher than that of the DFT-based method TD-B3LYP, which was about 1.5 h for acetone and 1 h for acetic acid using two Intel Xeon E5-2697 v2 CPUs. Our program has been highly developed for massive parallel calculations using both message passing interface (MPI) and OpenMP. We confirmed that the *GW* part of our program scales almost linearly up to 1536 MPI parallel executions in weak scaling measurement, and consequently, we can treat systems containing more than 100 atoms.[38]

RESULTS AND DISCUSSION

Figure 1 shows the XAS calculated for acetone and acetic acid together with the corresponding experimental spectra.[39,40] The detailed comparison with the experimental spectra is given in Table 1. It should be noted that for both acetone and acetic acid, the overall shapes of the experimental XAS spectra with low-energy sharp peaks and high-energy broad bands are similar to the calculated shapes. The first five excitons are labeled as S_n (n = 1−5), where S_1 has the lowest energy (the specific energies, relative oscillator strengths, and assignments are given in the Supporting Information). For simplicity, we use "exciton" for both bound excited states and Rydberg excitations (e.g., S_{3-5} of acetone). The lowest XAS peaks, at 531.4 eV for acetone and 532.13 eV for acetic acid, are close to the calculated S_1 peaks at 533.76 and 534.74 eV, respectively, and are blue-shifted by only 2.5 eV or 0.5% of the peak energy without any adjustable parameters. For the second-lowest XAS peaks, at 535.6 eV for acetone and 535.4 eV for acetic acid, the blue shifts of the corresponding calculated peaks at 544.17 eV (S_5) and 540.34 eV (S_3) are larger (about 5−9 eV). Consistent

DOI: 10.1021/acs.jctc.5b00082
J. Chem. Theory Comput. 2015, 11, 1668−1673

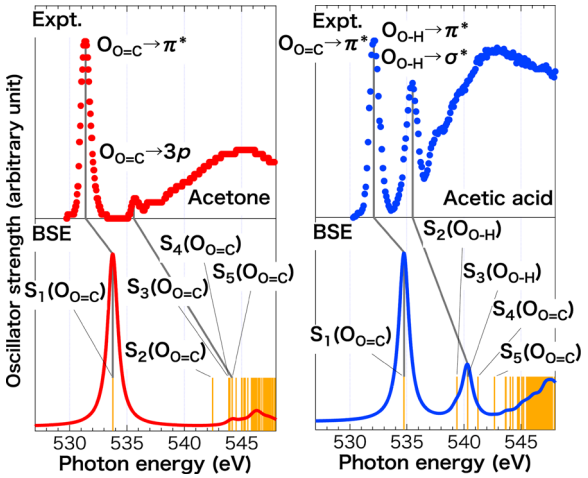

Figure 1. Oxygen 1s XAS calculated by BSE for acetone (red line) and acetic acid (blue line). The orange vertical bars at the bottom of the figure show individual excitations. The calculated spectra are directly compared to the experimental ones without any artificial shift (acetone, red dots; acetic acid, blue dots).[39,40] The experimental assignment was performed with the DFT-based method described in refs 39−41.

with trends in the experimental data, S_1 of acetic acid has a higher photon energy than that of acetone. The good agreement between the experimental results and our present calculations proves that the present *GW*+Bethe−Salpeter method is very useful for core electron excitations as well as for valence electron excitations, which have been previously studied in detail.[29,32]

In the XAS experiment for acetone in ref 39, the large first peak at 531.4 eV and the small second peak at 535.6 eV were assigned to $O_{O=C}$ 1s → π^* and $O_{O=C}$ 1s → 3p by comparison with DFT calculations based on the one-particle picture.[42,43] In our calculated results, they are assigned to the first and second dipole-allowed excitons, which are S_1 (533.76 eV) and S_5 (544.17 eV). Here S_1 is composed of a single dominant transition to the lowest unoccupied molecular orbital (LUMO) (=π^*) with a 97.4% contribution, which supports the previous one-particle-picture-based assignment. On the other hand, S_5 consists of transitions to LUMO+4 (=3p) and many other mixed states, where the contribution of LUMO+4 (=3p) is only 36.5%. This assignment emphasizes the importance of the strong excitonic effect, where multiple molecular orbitals are mixed with large weights via the Coulomb interaction in composing one exciton to form a transition peak.

In the XAS experiment for acetic acid, the first peak at 532.13 eV was assigned to $O_{O=C}$ 1s → π^*, and the second peak at 535.44 eV was assigned to O_{O-H} 1s → σ^* and π^* on the basis of a comparison with DFT calculations.[40,41] In a previous electron energy loss spectroscopy study,[44] the first peak was assigned to $O_{O=C}$ 1s →π^*, while the second peak was assigned to $O_{O=C}$ 1s → 3p and O_{O-H} 1s → π^* on the basis of term-value estimations. In our present calculation, the first peak corresponds to S_1, which is 97.3% composed of $O_{O=C}$ 1s → LUMO (=π^*), in agreement with the previous assignments. On the other hand, the experimental second peak corresponds to three excitons, labeled as S_2 (barely bright, 539.54 eV), S_3 (bright, 540.34 eV), and S_4 (dark, 541.22 eV). It should be noted that S_3 is an exciton consisting of a single dominant O_{O-H} 1s → LUMO (=π^*) transition, while S_2 consists of O_{O-H} 1s → LUMO+1 (=σ^*) and many other mixed states, where the contribution of LUMO+1 (=σ^*) is only 37.4%. This observation strongly suggests the failure of the one-particle picture[40,41] and indicates the importance of the strong excitonic effect. Although it is a fact that in the present results in particular the peak positions have a discrepancy with the experimental XAS by a few electron volts, as confirmed in Figure 1, our conclusion here is that the consideration of the two-particle picture is crucial in simulating the XAS as well as the case when the valence electron excitations are invariable.

Before comparing the excitation energy to those obtained using other calculation methods, we first mention the basis set dependence of unbound empty levels. Figure 2 shows the difference in the LDA Kohn−Sham orbitals of the empty states obtained with the all-electron mixed basis (PWs + AOs) and aug-cc-pVTZ (AOs only). The LDA Kohn−Sham orbitals up to the LUMO levels are consistent between these basis sets, although the orbitals for occupied states are not shown; however, the characteristics at higher levels are different, and the order changes at some levels (see Figure 2; corresponding orbitals are connected by lines). These differences primarily result from the poor description of the unbound empty states by the AO-only basis set. This basis set dependence is also seen in terms of the excitation energy.

Next we discuss the individual excitons in detail. Table 1 compares the excitation energies corresponding to S_1 for acetone and S_1 and S_3 for acetic acid to the experimental values.[39,40] We also performed TDDFT calculations with the LDA and Becke three-parameter Lee−Yang−Parr (B3LYP) exchange−correlation functionals,[45] and the values are listed in the "TD-LDA" and "TD-B3LYP" columns, respectively, for comparison. Here the values in the "LDA" and "GWA" columns are the excitation energies obtained from the

Table 1. Excitation Energies (in eV) Corresponding to the Transition from the Oxygen 1s Orbital to the LUMO (=π^*) Calculated with LDA, GWA, BSE, TD-LDA, and TD-B3LYP Are Listed Together with the Available Experimental Data[39,40,a]

	all-electron mixed basis			aug-cc-pVTZ		
	LDA	GWA	BSE	TD-LDA	TD-B3LYP	exptl[34,35]
acetone S_1 ($O_{O=C}$)	505.56	548.49	533.76	504.76	517.00	531.4
acetic acid S_1 ($O_{O=C}$)	505.80	548.70	534.74	505.34	519.15	532.13
acetic acid S_3 (O_{O-H})	507.26	550.32	540.34	506.64	520.43	535.44
relative value 1	0.24	0.21	0.98	0.58	2.15	0.73
relative value 2	1.46	1.62	5.64	1.30	1.28	3.31

[a]The experimental value for acetone was determined from the top of the first peak in ref 39. "Relative value 1" indicates the difference between acetone S_1 ($O_{O=C}$) and acetic acid S_1 ($O_{O=C}$), while "relative value 2" indicates the difference between acetic acid S_1 ($O_{O=C}$) and acetic acid S_3 (O_{O-H}).

DOI: 10.1021/acs.jctc.5b00082
J. Chem. Theory Comput. 2015, 11, 1668−1673

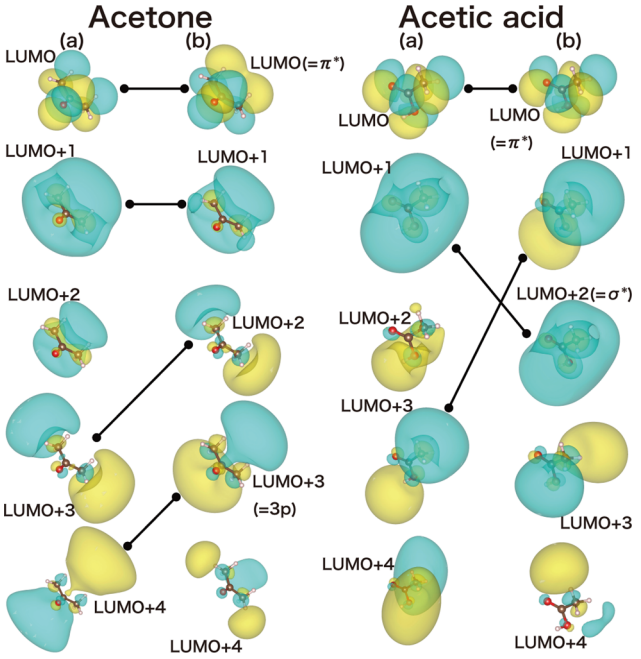

Figure 2. LDA Kohn–Sham orbitals obtained from (a) the all-electron mixed basis (PWs + AOs) and (b) aug-cc-pVTZ (AOs only). Corresponding orbitals are connected by lines.

difference between the orbital energies of the oxygen 1s orbital and the LUMO. Moreover, the excitation energies in the "BSE," "TD-LDA," and "TD-B3LYP" columns consider the excitonic effect in different ways.

In valence electron excitations, the LDA highest-occupied molecular orbital (HOMO)–LUMO gap becomes close to the experimental excitation energy value because two fatal errors in LDA, i.e., the small HOMO–LUMO gap and the lack of an excitonic effect, have almost same value and can accidentally cancel out. However, this accidental cancellation does not occur in the core electron region, so the values in the "LDA" column are about 25–28 eV less than the experimental data. This suggests that the LDA Kohn–Sham orbital energies at the oxygen 1s level are strongly underestimated. Because the absolute values are large, the *GW* correction is also large. The *GW* gaps are about 43 eV larger than those of LDA. However, because of the lack of an excitonic effect, the values still differ from the experimental values by approximately 10–17 eV.

The TDDFT and BSE methods consider excitonic effects with different electron–hole interaction kernels. TDDFT is known to be well-balanced between accuracy and the required computational cost in studying low-energy excitations. However, the TDDFT correction, including the local excitonic effects in both space and time, is obviously insufficient for high-energy excitations involving core electrons. The discrepancies from the experimental data are about 27–29 eV (or 5% error) for TD-LDA and 13–15 eV (or 2.4–2.8% error) for TD-B3LYP.

To handle the strong excitonic effect involving the oxygen 1s orbital, the nonlocal, dynamic excitonic effects through the *GW* electron–hole interaction kernel must be considered. Here we confirm the strong excitonic effect in terms of the exciton binding energies, defined as the difference between the values in the "BSE" and "GWA" columns. These differences are about 10 eV or more, which is obviously much larger than the case of valence electron excitation. The best results in Table 1 occur with the BSE method. The remaining errors are only about 2.4 eV for acetone and 2.5–4.8 eV for acetic acid (the origin of these errors is discussed in the next paragraph). These discrepancies are less than 1% of the absolute values. Consequently, our method drastically improves TDDFT errors.

Apart from the discussion of the absolute values, we also mention two relative values in Table 1. Discussion based on relative values is sometimes preferred, especially for (semi)-empirical or low-reliability methods, where the relative value is the only way to compare with the experimental data or other simulation results. In the following section, we define "relative value 1" as the difference between acetone S_1 ($O_{O=C}$) and acetic acid S_1 ($O_{O=C}$), while "relative value 2" is the difference between acetic acid S_1 ($O_{O=C}$) and acetic acid S_3 (O_{O-H}). These relative values show a quite different aspect compared with the absolute values. In fact, the TD-LDA value is closer to the experimental one than TD-B3LYP and BSE for both "relative value 1" and "relative value 2," while TD-B3LYP shows a larger discrepancy with the experimental value than BSE for "relative value 1" and a smaller discrepancy for "relative value 2." In addition, the best value for "relative value 2" is GWA, and the second best is LDA. These comparisons demonstrate a widely known empirical fact that TD-LDA calculations, which have small computational costs, very often provide good matches to experimental data concerning the relative peak positions. As for theoretical approximation levels, it is known that TD-B3LYP is better than TD-LDA and that BSE is better than GWA. In Table 1, the absolute values follow this order while the relative values are in the reverse order. Theoretical validations for the good matches in relative values have not been provided and remain unanswered.

Next we discuss the strong excitonic effect. Figure 3 visually shows the hybridizations for low-lying isolated excitons (also

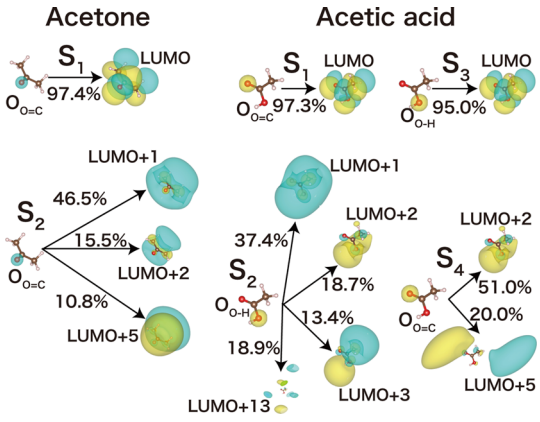

Figure 3. LDA Kohn–Sham orbitals involved in isolated excitons near the band-edge states. Strong hybridizations among transitions are confirmed at S_2 for acetone and S_2 and S_4 for acetic acid. The contributions (in %) of each transition are also given.

see the Supporting Information). For both molecules, the LUMO is the only bound state localized around the molecule as a π-type orbital, and all of the higher empty levels are unbound states, e.g., Rydberg states weakly localized around molecules or free electron states expanding in the whole unit cell. Therefore, S_1 for acetone and S_1 and S_3 for acetic acid corresponding to the transition to the LUMO show weak hybridization, i.e., the single transition to the LUMO is the dominant contribution. Moreover, other excitons (e.g., S_2 for

DOI: 10.1021/acs.jctc.5b00082
J. Chem. Theory Comput. 2015, 11, 1668–1673

acetone and S_2 and S_4 for acetic acid) are composed of multiple transition states as a result of strong mixing. This fact can be identified because an easy assignment based on the one-particle picture (or one-particle approximation) is misleading for these excitons. In actuality, our assignments are consistent with those of refs 39−41 for a single dominant transition to the LUMO (e.g., S_1 of both molecules). However, our assignments differ for other excitons where multiple transitions intricately contribute. The assignments for excitons in the broad peaks of both molecules and at the second peak of acetic acid are symbolic results that confirm the difference between BSE and the simple assignment based on the one-particle picture in refs 39−41. In such cases, the one-particle picture is collapsed for the core electron excitations and, similar to the case of valence electron excitations, an advanced method based on the two-particle picture, i.e., our BSE method, would be required.

To improve the present method in a future study, we speculate two reasons for the present errors in our comparison of absolute values (see Table 1). One possibility is the limitation of GWA in describing the deep-core electron states. While GWA is a well-established and accurate method in the valence electron region, *GW* quasiparticle energies are accurate for experimental first ionization potentials and electron affinities. However, this accuracy might be an open question in the core electron region. If it is true that GWA is the origin of the present error, we need to consider higher-order exchange terms. (This is also significant for explicitly removing the self-interaction effect.) Another concern in our method might be related to the accuracy of LDA, in particular to the accuracy of the LDA Kohn−Sham orbitals. As we already know, LDA has some problems in the treatment of strongly correlated materials. For example, LDA fails to describe the strongly localized states of the Mott insulator, and consequently, the Mott insulator is described as a metal system in LDA calculations.[46] A similar problem may occur in the description of the core electron states, which are strongly localized around the nucleus. (It should be noted that if we assume nonoverlapping atomic spheres, the amplitudes of the LDA Kohn−Sham orbitals at the core levels (e.g., O 1s in the present case) have nonzero values only inside the atomic sphere. Although the LDA Kohn−Sham orbitals at the core levels are well-localized in this sense, the exact orbitals are expected to be localized at the nucleus more strongly than that of LDA.) In either case, we need more practical calculations to explicitly define the errors. The present study is one step toward the further development of this methodology, and we believe that the speculation provided here can be useful for future developments.

SUMMARY

We have investigated the oxygen 1s XAS of acetone and acetic acid molecules using the first-principles *GW*+Bethe−Salpeter method employing the all-electron mixed-basis approach. The calculated XAS were compared to available experimental data in terms of the peak positions and peak heights. The remaining errors for the first peak position were only about 2.4 eV for acetone and 2.5 eV for acetic acid, corresponding to errors of less than 1% from the experimental values. This is a significant improvement from that of TDDFT (5% error (27−29 eV) for TD-LDA and 2.4−2.8% error (13−15 eV) for TD-B3LYP). We have assigned the first five excitons and noted that simple methods based on the one-particle picture are invalid for fully analyzing or simulating the experimental spectra. This combination of the *GW*+Bethe−Salpeter method and the all-electron mixed-basis approach handles the XAS simulation with accuracy and computational efficiency. The excitation energies simulated from first principles in this study have somewhat larger deviations from those of experiments; we believe that providing such inconvenient information is significant and worthwhile for further theoretical development. The present study has opened new possibilities for studying high-energy excitation involving X-rays and core electrons from first principles. On the basis of the past successes of *GW*+Bethe−Salpeter calculations for valence excitations, our method is potentially capable of simulating XAS for a wide range of materials, from isolated and extended systems to liquid systems as well as covalent-, metallic-, ionic-, and hydrogen-bonding systems. In a future study, the present method could be valid for simulating core excitations in dissolved molecules where strong state hybridization plays an important role.

ASSOCIATED CONTENT

Supporting Information

Complete ref 45 and detailed exciton profiles of acetone and acetic acid. This material is available free of charge via the Internet at http://pubs.acs.org.

AUTHOR INFORMATION

Corresponding Author

*E-mail: y.noguchi@issp.u-tokyo.ac.jp.

Funding

Y.N. was supported by a Grant-in-Aid for Young Scientist (B) (23740288) and a Grant-in-Aid for Scientific Research (C) (26400383) from the Japan Society for the Promotion of Science (JSPS). This work was partially supported by KAKENHI (23360135 and 26610081) from JSPS, the Photon Frontier Network Program of MEXT, JST-CREST, and JST-SENTSN in Japan.

Notes

The authors declare no competing financial interest.

ACKNOWLEDGMENTS

The present calculations were performed with supercomputers from the Institute for Solid State Physics, University of Tokyo; the Information Technology Center, University of Tokyo; the Research Institute for Information Technology, Kyushu University; and the Information Technology Center, Nagoya University.

REFERENCES

(1) Stöhr, J. Selected Applications of NEXAFS. *Springer Ser. Surf. Sci.* **1992**, *25*, 292−341.

(2) de Groot, F. M. F. High-Resolution X-ray Emission and X-ray Absorption Spectroscopy. *Chem. Rev.* **2001**, *101*, 1779−1808.

(3) Triguero, L.; Pettersson, L. G. M.; Ågren, H. Calculations of Near-Edge X-ray-Absorption Spectra of Gas-Phase and Chemisorbed Molecules by Means of Density-Functional and Transition-Potential theory. *Phys. Rev. B* **1998**, *58*, 8097−8110.

(4) Sun, Y. P.; Hennies, F.; Pietzsch, A.; Kennedy, B.; Schmitt, T.; Strocov, V. N.; Andersson, J.; Berglund, M.; Rubensson, J. E.; Aidas, K.; Gel'mukhanov, F.; Odelius, M.; Föhlisch, A. Intramolecular Soft Modes and Intermolecular Interactions in Liquid Acetone. *Phys. Rev. B* **2011**, *84*, No. 132202.

(5) Leetmaa, M.; Ljungberg, M. P.; Lyubartsev, A.; Nilsson, A.; Pettersson, L. G. M. Theoretical Approximations to X-ray Absorption Spectroscopy of Liquid Water and Ice. *J. Electron Spectrosc. Relat. Phenom.* **2010**, *177*, 135−157.

DOI: 10.1021/acs.jctc.5b00082
J. Chem. Theory Comput. 2015, 11, 1668−1673

(6) Takahashi, O.; Pettersson, L. G. M. Functional Dependence of Core-Excitation Energies. *J. Chem. Phys.* **2004**, *121*, 10339−10345.
(7) Kolczewski, C.; Püttner, R.; Plashkevych, O.; Ågren, H.; Staemmler, V.; Martins, M.; Snell, G.; Schlachter, A. S.; ant'Anna, M.; Kaindl, G.; Pettersson, L. G. M. Detailed Study of Pyridine at the C 1s and N 1s Ionization Thresholds: The Influence of the Vibrational Fine Structure. *J. Chem. Phys.* **2001**, *115*, 6426−6437.
(8) Ågren, H.; Carravetta, V.; Vahtras, O.; Pettersson, L. G. M. Direct, Atomic Orbital, Static Exchange Calculations of Photoabsorption Spectra of Large Molecules and Clusters. *Chem. Phys. Lett.* **1994**, *222*, 75−81.
(9) Besley, N. A.; Asmuruf, F. A. Time-dependent density functional theory calculations of the spectroscopy of core electrons. *Phys. Chem. Chem. Phys.* **2010**, *12*, 12024−12039.
(10) Mangione, G.; Sambi, M.; Nardi, M. V.; Casarin, M. A Theoretical Study of the L_3 Pre-Edge XAS in Cu(II) Complexes. *Phys. Chem. Chem. Phys.* **2014**, *16*, 19852−19855.
(11) Song, J.-W.; Watson, M. A.; Nakata, A.; Hirao, K. Core-excitation energy calculations with a long-range corrected hybrid exchange−correlation functional including a short-range Gaussian attenuation (LCgaus-BOP). *J. Chem. Phys.* **2008**, *129*, No. 184113.
(12) Hybertsen, M. S.; Louie, S. G. Electron Correlation in Semiconductors and Insulators: Band Gaps and Quasiparticle Energies. *Phys. Rev. B* **1986**, *34*, 5390−5413.
(13) Blase, X.; Attaccalite, C.; Olevano, V. First-Principles *GW* Calculations for Fullerenes, Porphyrins, Phtalocyanine, and Other Molecules of Interest for Organic Photovoltaic Applications. *Phys. Rev. B* **2011**, *83*, No. 115103.
(14) Rohlfing, M.; Louie, S. G. Electron−Hole Excitations and Optical Spectra from First Principles. *Phys. Rev. B* **2000**, *62*, 4927−4944.
(15) Rohlfing, M. Redshift of Excitons in Carbon Nanotubes Caused by the Environment Polarizability. *Phys. Rev. Lett.* **2012**, *108*, No. 087402.
(16) Sham, L. J.; Rice, T. M. Many-Particle Derivation of the Effective-Mass Equation for the Wannier Exciton. *Phys. Rev.* **1966**, *144*, 708−714.
(17) Strinati, G. Effects of Dynamical Screening on Resonances at Inner-Shell Thresholds in Semiconductors. *Phys. Rev. B* **1984**, *29*, 5718−5726.
(18) Hedin, L. New Method for Calculating the One-Particle Green's Function with Application to the Electron-Gas Problem. *Phys. Rev.* **1965**, *139*, A796−A823.
(19) Shirley, E. L. Ti 1s Pre-Edge Features in Rutile: A Bethe−Salpeter Calculation. *J. Electron Spectrosc. Relat. Phenom.* **2004**, *136*, 77−83.
(20) Shirley, E. L. Direct SCF Direct Static-Exchange Calculations of Electronic Spectra. *J. Electron Spectrosc. Relat. Phenom.* **2005**, *144−147*, 1187−1190.
(21) Vinson, J.; Rehr, J. J.; Kas, J. J.; Shirley, E. L. Bethe−Salpeter equation calculations of core excitation spectra. *Phys. Rev. B* **2011**, *83*, No. 115106.
(22) Vinson, J.; Rehr, J. J. Ab initio Bethe−Salpeter calculations of the X-ray absorption spectra of transition metals at the L-shell edges. *Phys. Rev. B* **2012**, *86*, No. 195135.
(23) Vinson, J.; Rehr, J. J. Ab Initio Bethe−Salpeter Calculations of the X-Ray Absorption Spectra of Transition Metals at the L-Shell Edge. *Phys. Rev. B* **2012**, *86*, 195135/1−195135/6.
(24) Vinson, J.; Kas, J. J.; Vila, F. D.; Rehr, J. J.; Shirley, E. L. Theoretical Optical and X-ray Spectra of Liquid and Solid H_2O. *Phys. Rev. B* **2012**, *85*, No. 045101.
(25) Rehr, J. J. Theory and calculations of X-ray spectra: XAS, XES, XRS, and NRIXS. *Radiat. Phys. Chem.* **2006**, *75*, 1547.
(26) Shirley, E. L. Ab initio Inclusion of electron−hole attraction: Application to X-ray absorption and resonant inelastic X-ray scattering. *Phys. Rev. Lett.* **1998**, *80*, 794−797.
(27) Ono, S.; Noguchi, Y.; Sahara, R.; Kawazoe, Y.; Ohno, K. TOMBO: All-electron mixed-basis approach to condensed matter physics. *Comput. Phys. Commun.* **2015**, *189*, 20−30.
(28) Herman, F.; Skillman, S. *Atomic Structure Calculations*; Prentice Hall: Englewood Cliffs, NJ, 1963.
(29) Noguchi, Y.; Ohno, K. All-Electron First-Principles *GW* +Bethe−Salpeter Calculation for Optical Absorption Spectra of Sodium Clusters. *Phys. Rev. A* **2010**, *81*, No. 045201.
(30) Noguchi, Y.; Ohno, K.; Solovyev, I.; Sasaki, T. Cluster size dependence of double ionization energy spectra of spin-polarized aluminum and sodium clusters: All-electron spin-polarized *GW*+*T*-matrix method. *Phys. Rev. B* **2010**, *81*, No. 165411.
(31) Noguchi, Y.; Sugino, O.; Nagaoka, M.; Ishii, S.; Ohno, K. A *GW* +Bethe−Salpeter Calculation on Photoabsorption Spectra of $(CdSe)_3$ and $(CdSe)_6$ Clusters. *J. Chem. Phys.* **2012**, *137*, No. 024306.
(32) Noguchi, Y.; Sugino, O.; Okada, H.; Matsuo, M. First-Principles Investigation on Structural and Optical Properties of $M^+@C_{60}$ (Where M = H, Li, Na, and K). *J. Phys. Chem. C* **2013**, *117*, 15362.
(33) Noguchi, Y.; Hiyama, M.; Akiyama, H.; Koga, N. First-Principles Investigation on Rydberg Excitations of Firefly Luciferin Anion in Vacuum. *J. Chem. Phys.* **2014**, *141*, No. 044309.
(34) Coriani, S.; Christiansen, O.; Fransson, T.; Norman, P. Coupled-cluster response theory for near-edge X-ray-absorption fine structure of atoms and molecules. *Phys. Rev. A* **2012**, *85*, No. 022507.
(35) Since actual calculations with all-electron methods employing localized AOs often employ Gaussian-type orbitals (GTOs), expressed by $e^{-\alpha r^2}$, such AO-only methods fail to describe the cusp condition.[47] In addition, AO-only methods are intrinsically unable to describe extremely delocalized states such as the free electron states above the vacuum level.
(36) Castro, A.; Rubio, A.; Stott, M. J. Solution of Poisson's Equation for Finite Systems Using Plane-Wave Methods. *Can. J. Phys.* **2003**, *81*, 1151−1164.
(37) Rozzi, C. A.; Varsano, D.; Marini, A.; Gross, E. K. U.; Rubio, A. Exact Coulomb Cutoff Technique for Supercell Calculations. *Phys. Rev. B* **2006**, *73*, No. 205119.
(38) Noguchi, Y.; Sugino, O. Symmetry breaking and excitonic effects on optical properties of defective nanographenes. *J. Chem. Phys.* **2015**, *142*, No. 064313.
(39) Tamenori, Y.; Takahashi, O.; Yamashita, K.; Yamaguchi, T.; Okada, K.; Tabayashi, K.; Gejo, T.; Honma, K. Hydrogen bonding in acetone clusters probed by near-edge X-ray absorption fine structure spectroscopy in the carbon and oxygen K-edge regions. *J. Chem. Phys.* **2009**, *131*, No. 174311.
(40) Tabayashi, K.; Yamamoto, K.; Maruyama, T.; Yoshida, H.; Okada, K.; Tamenori, Y.; Suzuki, I. H.; Gejo, T.; Honma, K. Core-electron excitation and fragmentation processes of hydrogen bonded acetic-acid clusters in oxygen K-edge region. *J. Electron Spectrosc. Relat. Phenom.* **2011**, *184*, 134−139.
(41) Tabayashi, K.; Takahashi, O.; Namatame, H.; Taniguchi, M. Substituent R-effects on the core-electron excitation spectra of hydrogen-bonded carboxylic-acid (R−COOH) clusters: Comparison between acetic-acid and formic-acid clusters. *Chem. Phys. Lett.* **2013**, *557*, 1−9.
(42) Prince, K. C.; Richter, R.; de Simone, M.; Alagia, M.; Coreno, M. Near Edge X-ray Absorption Spectra of Some Small Polyatomic Molecules. *J. Phys. Chem. A* **2003**, *107*, 1955−1963.
(43) Yang, L.; Ågren, H. Static Exchange and Quantum Defect Analysis of X-ray Absorption Spectra of Carbonyl Compounds. *Phys. Scr.* **1996**, *54*, 614−624.
(44) Robin, M. B.; Ishii, I.; Mclaren, R.; Hitchcock, A. P. Fluorination Effects on the Inner-Shell Spectra of Unsaturated Molecules. *J. Electron Spectrosc. Relat. Phenom.* **1988**, *47*, 53−92.
(45) Frisch, M. J.; et al. *Gaussian 09*, revision C.01; Gaussian, Inc.: Wallingford, CT, 2009.
(46) Ohno, K.; Noguchi, Y.; Yokoi, T.; Ishii, S.; Takeda, J.; Furuya, M. Significant Reduction of On-Site Coulomb Energy *U* due to Short-Range Correlation in an Organic Mott Insulator. *ChemPhysChem* **2006**, *7*, 1820−1824.
(47) Pachucki, K.; Komasa, J. Gaussian basis sets with the cusp condition. *Chem. Phys. Lett.* **2004**, *389*, 209−211.

DOI: 10.1021/acs.jctc.5b00082
J. Chem. Theory Comput. 2015, 11, 1668−1673